

Multi-functional properties of $\text{CaCu}_3\text{Ti}_4\text{O}_{12}$ thin films

A. A. Felix, J. L. M. Rupp, J. A. Varela, and M. O. Orlandi

Citation: *J. Appl. Phys.* **112**, 054512 (2012); doi: 10.1063/1.4751344

View online: <http://dx.doi.org/10.1063/1.4751344>

View Table of Contents: <http://jap.aip.org/resource/1/JAPIAU/v112/i5>

Published by the [AIP Publishing LLC](#).

Additional information on *J. Appl. Phys.*

Journal Homepage: <http://jap.aip.org/>

Journal Information: http://jap.aip.org/about/about_the_journal

Top downloads: http://jap.aip.org/features/most_downloaded

Information for Authors: <http://jap.aip.org/authors>

ADVERTISEMENT



AIP Advances

Now Indexed in
Thomson Reuters
Databases

Explore AIP's open access journal:

- Rapid publication
- Article-level metrics
- Post-publication rating and commenting

Multi-functional properties of $\text{CaCu}_3\text{Ti}_4\text{O}_{12}$ thin films

A. A. Felix,^{1,2} J. L. M. Rupp,² J. A. Varela,¹ and M. O. Orlandi^{1,a)}

¹*Departamento de Físico-Química, Instituto de Química, Universidade Estadual Paulista, Araraquara, São Paulo 14800-900, Brazil*

²*Department of Materials Science and Engineering, Massachusetts Institute of Technology, Cambridge, Massachusetts 02139, USA*

(Received 9 May 2012; accepted 9 August 2012; published online 13 September 2012)

In this work, electric transport properties of $\text{CaCu}_3\text{Ti}_4\text{O}_{12}$ (CCTO) thin films were investigated for resistive switching, rectifying and gas sensor applications. Single phase CCTO thin films were produced by polymeric precursor method (PPM) on different substrates and their electrical properties were studied. Films produced on LNO/Si substrates have symmetrical non-ohmic current-voltage characteristics, while films deposited on Pt/Si substrates have a highly asymmetrical non-ohmic behavior which is related to a metal-semiconductor junction formed at the CCTO/Pt interface. In addition, results confirm that CCTO has a resistive switching response which is enhanced by Schottky contacts. Sensor response tests revealed that CCTO films are sensitive to oxygen gas and exhibit n-type conductivity. These results demonstrate the versatility of CCTO thin film prepared by the PPM method for gas atmosphere or bias dependent resistance applications. © 2012 American Institute of Physics. [<http://dx.doi.org/10.1063/1.4751344>]

I. INTRODUCTION

In the last decade, materials with high dielectric constant have been thoroughly researched due to their potential applications in microelectronic devices. Recently, $\text{CaCu}_3\text{Ti}_4\text{O}_{12}$ (CCTO) has attracted scientific interest due to its huge dielectric constant^{1–7} and hysteretic current-voltage profile^{8–12} for applications in electronic devices such as random access memories, microwave devices, sensors, etc.^{1–19} However, CCTO applications in microelectronic devices such as sensors or random access memories lead to the integration of this oxide in the form of thin films on silicon-based substrates. Several studies of CCTO thin films prepared by different methods have shown that this material has multi-functional properties which are directly related to the synthesis route and the electrode/substrate used. Deng *et al.*^{13,14} reported current-voltage rectifying behavior in CCTO thin films prepared by pulsed laser deposition (PLD). They show that, due to a Cu-rich layer in the film surface, a metal-insulator-semiconductor (MIS) junction or a metal-semiconductor (MS) junction between the CCTO film and top electrode can be formed. CCTO thin films grown by *rf-sputtering* result in the formation of well-aligned nanorods depending on the substrate temperature.¹⁵ They display a resistive switching effect which is attributed to the polarization of defects at grain boundaries.¹¹ Hysteretic current-voltage was also observed in thin films prepared by chemical methods. Lin *et al.* showed that the conductivity in CCTO films prepared by the sol-gel method on Pt/Ti/SiO₂/Si substrates is strongly affected by the electrode/film interface due to the work function of the metal used as the top electrode.^{12,16} Gas sensing properties have also been reported by several researchers for CCTO thin films; however, the type

of conductivity in these films is not well defined in the literature. Kim *et al.*¹⁷ reported the preparation of macroporous CCTO thin films by PLD onto PMMA (polymethyl methacrylate) microsphere templated substrates. These films have n-type conductivity and higher H₂ sensitivity compared to CO and CH₄. N-type conductivity was also reported by Parra *et al.* in mesoporous thin films prepared by the sol-gel method.¹⁸ On the other hand, Joanni *et al.* showed that films prepared by *rf-sputtering* display p-type conductivity.¹⁹

In light of these predictions, the main goal of this study is to investigate the multi-functionality of CCTO thin films prepared by the polymeric precursor method (PPM). Electrode-CCTO film interfaces on non-linear charge transport and gas sensing were investigated, and their potential applications in micro-devices such as resistance random access memories, Schottky diodes, or gas sensors are discussed.

II. EXPERIMENTAL

A. Synthesis procedure

CCTO thin films were prepared by PPM on three different substrates: Si (111) with a LaNiO₃ (LNO) buffer layer, Al₂O₃ and Pt/TiO₂/SiO₂/Si (100). More details regarding the PPM were reported by Zanetti *et al.*²⁰ The molar ratio of metal: citric acid: ethylene glycol was 1:3:3 in both CCTO and LNO solutions. For the substrate with the buffer layer, the first step was to prepare the LNO electrodes on a Si (111) substrate. Stoichiometric amounts of lanthanum carbonate ((La₂CO₃)₃.xH₂O, Sigma-Aldrich, 99.99%) and nickel nitrate (Ni(NO₃)₂.6H₂O, Sigma-Aldrich, 99.99%) were dissolved in an aqueous nitric acid solution at 50 °C. After homogenization, citric acid was added to the solution to form metal chelates. Then the temperature was raised to 95 °C, and ethylene glycol was added to achieve the polymerization reaction. The viscosity of the resulting solution was adjusted to 30 cP by controlling the water content using a Brookfield viscosimeter.

^{a)}Author to whom correspondence should be addressed. Electronic mail: orlandi@iq.unesp.br. Tel.: +55 16 3301 9644. Fax: +55 16 3322 0015.

A LNO layer was deposited on a Si (111) substrate by spin coating at 4000 rpm for 30 s (Spin coater; Laurell Tech. Corp., Model WS-400B) followed by heat treatment at 370 °C for 4 h in a conventional oven to remove organic material; these steps were repeated three times, and finally thin films were annealed at 825 °C for 60 min in air.

To obtain CCTO films, calcium carbonate (CaCO_3 , Sigma-Aldrich, 99.999%), copper(II) carbonate basic ($\text{CuCO}_3 \cdot \text{Cu}(\text{OH})_2$, Sigma-Aldrich, 99.99%) and titanium(IV) isopropoxide ($\text{C}_{12}\text{H}_{28}\text{O}_4\text{Ti}$, Sigma-Aldrich, 99.999%) were used to prepare the CCTO solution. The precursor solution of Ca, Cu, and Ti atoms was prepared by adding raw materials to an aqueous citric acid/ethylene glycol solution with constant stirring and heating at 90 °C. Then the viscosity of the resulting solution was adjusted to 30 cP by controlling the water content. CCTO layers were deposited on substrates (alumina, LNO/Si and Pt/Si) by spin coating at 4000 rpm for 30 s followed by heat treatment at 370 °C for 4 h to remove the organic material. Three CCTO layers were deposited, and thin films were annealed after the whole process at 775 °C for 30 min in air.

B. Structural and morphological characterization

Phase analysis of CCTO thin films was performed by x-ray diffraction (XRD; Rigaku, Model Rint 2000) at room temperature. The annealed film thickness was analyzed using a field emission scanning electron microscope (FEG-SEM; JEOL, Model 7500F).

C. Electrical characterization

To perform electrical measurements, top electrodes (300 μm diameter) were deposited by Au sputtering through a shadow mask at room temperature in CCTO films prepared on LNO or Pt bottom electrodes. Electrical properties were measured by an Au/CCTO/bottom electrode capacitor structure. Current–voltage measurements were taken using a stabilized high voltage source measuring unit (Keithley, Model 237) with different time delay by point in the temperature range from 25 °C to 250 °C with a step of 25 °C. The Pt wires were used as probe electrodes.

D. Sensor response

CCTO films were deposited on Al_2O_3 substrates and interdigitated Au-electrodes (100 μm Au fingers spaced by 200 μm) were sputtered at room temperature on the CCTO film surface to characterize its sensor response. Sensing tests were performed at 200 °C, 250 °C, and 300 °C by applying a d.c. voltage of 20 V. The sensor response of CCTO thin films was performed by cyclic exposure to oxygen gas by varying the concentration between 12% and 0.05% in a nitrogen gas flow of 150 sccm. Resistance–time measurements were taken using a stabilized high voltage source measuring unit (Keithley, Model 237) with a delay of one second.

III. RESULTS AND DISCUSSION

Figure 1 shows XRD patterns for CCTO thin films grown on different substrates at 775 °C for 30 min. CCTO

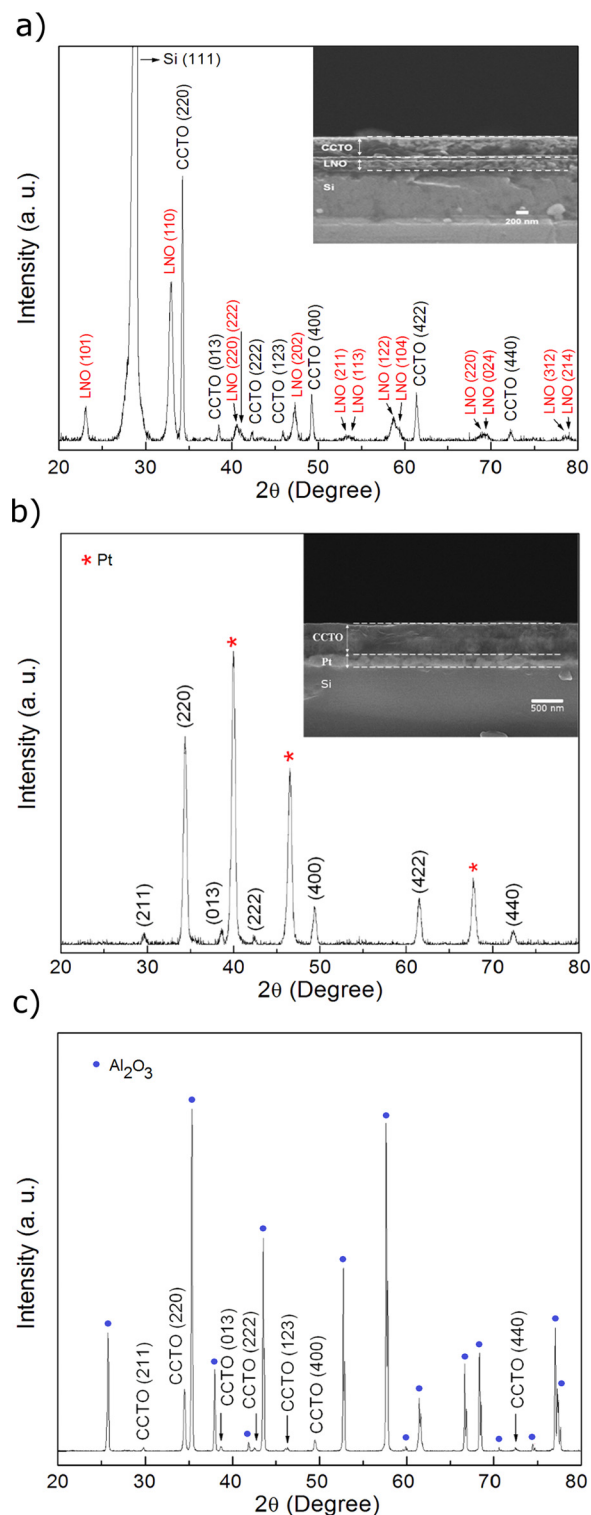


FIG. 1. XRD patterns of CCTO film grown on (a) LNO buffer, (b) Pt electrode, and (c) alumina substrate. The inset shows transversal section of the films.

peaks can be indexed for all samples by a cubic body-centered perovskite-related structure with space group $\text{Im}\bar{3}$ according to JCPDS 75-2188 and do not present any preferential orientation. Additional peaks of LaNiO_3 (JCPDS 79-2450), Pt (JCPDS 87-640), Si (111), and Al_2O_3 (JCPDS 71-225) related to the bottom electrodes and/or substrates were observed. LNO and CCTO layers can be seen in the

cross sectional images and present a high degree of densification and thickness around 250 nm and 450 nm, respectively (see Figure 1(a) inset). A high degree of densification and a thickness of 500 nm are also visible in the CCTO film grown on a Pt electrode (see Figure 1(b) inset).

In the following sections, the electrical characteristics of these three CCTO samples will be discussed. Sensor, rectifying and resistive switching behavior were tested for these samples.

A. Gas sensing response

The predominant electrical character of semiconductor oxides can be classified according to the resistance change direction relative to the oxidant atmosphere. This classification is related to the intrinsic conductivity type of semiconductor oxides which is determined by the nature of the dominant charge carriers; i.e., electrons or holes. If the material resistance increases when the film is exposed to an oxidant atmosphere, the oxide has n-type conductivity; if the material resistance decreases when the film is exposed to an oxidant atmosphere, the oxide has p-type conductivity.^{21,22} In addition, the conductance in n-type semiconductor oxides is dependent on oxygen partial pressure, and it decreases when the oxygen partial pressure increase (the inverse is valid for p-type semiconductor oxides).^{23,24} Based on these fundamentals, sensor measurements were performed to determine the dominant charge carriers for CCTO films prepared by the PPM and to verify the gas sensitivity of the material (sensor characteristics). The gas test was performed with an oxygen concentration at 12% and varying operating temperatures (200 °C, 250 °C, and 300 °C) (see Figure 2).

The sensor signal of CCTO thin films increases when the film is exposed to an oxygen atmosphere (the resistance in oxygen is higher than in nitrogen) which indicates that CCTO films reveal predominant n-type (electronic) conductivity for the PPM processing. The sensor response as a function of oxygen partial pressure was measured at 300 °C (see Figure 3). The sensor signal depends on the oxygen partial pressure, and the resistance increases when the oxygen concentration increases (see Figure 3 inset). This result corroborates

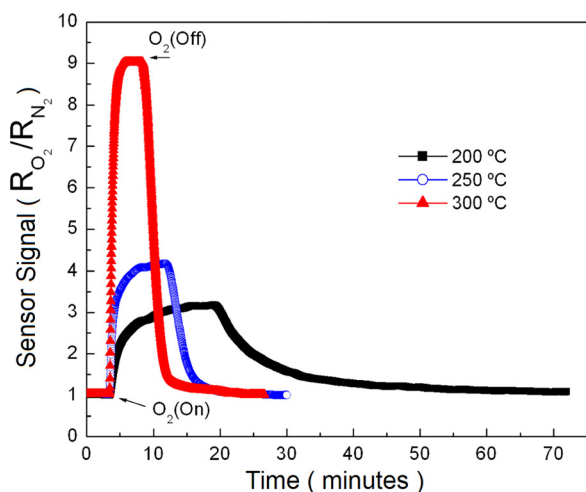


FIG. 2. Sensor signal vs. time for different temperatures at 12% oxygen partial pressure.

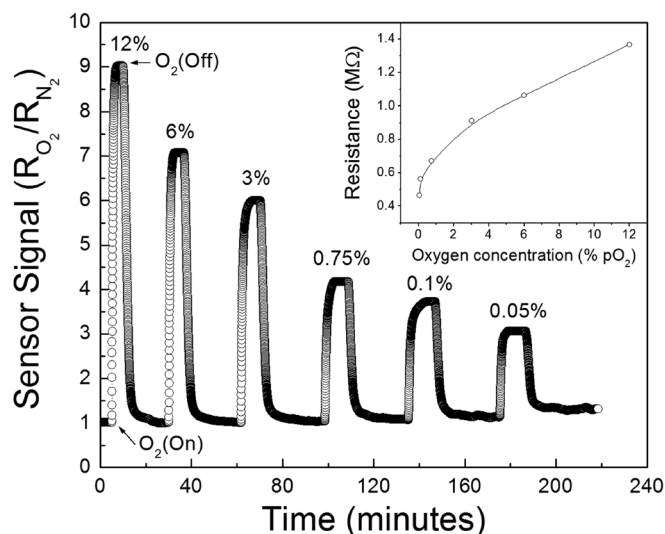


FIG. 3. Sensor signal vs. time for different oxygen partial pressure at 300 °C. The inset shows the resistance as a function of oxygen concentration.

the n-type charge carrier of CCTO thin film prepared by the PPM. These results agree with the results obtained by Parra *et al.* for CCTO films prepared by the sol-gel method which is a synthesis procedure similar to our method.¹⁸ In addition, thermopower measurements (not shown here) were performed which indicate a negative Seebeck coefficient (S) and verify the n-type conductivity in our CCTO thin films.²⁵ On the other hand, p-type conductivity was observed by thin films deposited by vacuum-based film processing such as PLD.^{13,19} It may be hypothesized that either organic residues from wet-chemical processing or gas environments in the physical processing (PLD or sputtering) can affect the near-ordering of the thin film CCTO phase due to the oxygen partial pressure during the synthesis procedure. Examples are reported in the literature for ceria- and zirconia-based thin films where the near-ordering of oxygen-cation bonds can be substantially affected by the initial processing route.^{26–28} Thus, this singularity in CCTO thin films is not completely understood and is still an open research topic.

B. Rectifying behavior

In order to study the barrier contacts formed on the electrodes/film interface, CCTO thin films were prepared by the PPM on conductive (LaNiO_3) and metal (Au and Pt) electrodes, and current-voltage characteristics were measured. All samples were measured using Au as the top electrode and LaNiO_3 or Pt as bottom electrodes. Figure 4 shows the non-cyclic current vs. voltage curves for the CCTO film prepared on the Au/CCTO/Pt set-up up to $10 \mu\text{A}$, and the inset shows current-voltage profiles for Au/CCTO/Pt and Au/CCTO/LNO set-ups. LNO film has a resistivity of around $5 \times 10^{-4} \Omega \text{ m}$ which is suitable as a bottom electrode for electrical measurements. The non-linear behavior of the current observed in the CCTO film prepared on LNO indicates Schottky-type conductivity, typically observed in this material, with non-linear coefficient (α) of about 2.^{29,30} Moreover, the symmetry of I vs. V curves in forward and reverse voltages was expected since that LNO phase displays a n-type

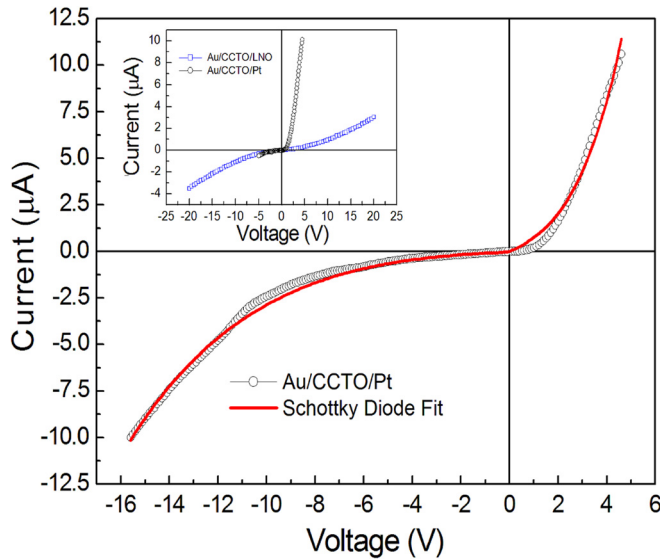


FIG. 4. Current-voltage curve of the Au/CCTO/Pt setup at room temperature. The applied voltage was from +5 V to -16 V up to 10 μA . The solid red line over the experimental data is the theoretical simulation of the Schottky thermionic emission equation. The left inset shows the current-voltage curve for Au/LNO/CCTO and Au/CCTO/Pt set-ups.

conductivity which forms an ohmic contact with perovskite materials.^{31,32} The Au top electrode has a work function value very close to the CCTO electron affinity which also forms an ohmic contact (as discussed below).

Rectifying behavior for a CCTO film prepared on a Pt-electrode is characterized by strong asymmetry in the current vs. voltage curves. This film possesses a good rectifying characteristic for low reverse voltages (see inset in Figure 4) with the current increasing slowly ($\alpha \approx 1$) as a function of applied voltage up to 10 μA . However, for forward voltages the current increases more abruptly ($\alpha \approx 7$), evidencing the rectifying behavior of the sample. Zang *et al.* proposed that CCTO has an intrinsic back-to-back Schottky barrier at grain boundaries and it was recently confirmed by using d.c. characterizations.^{33,34} Nevertheless, we do not believe that the asymmetric response in I vs V curves is an intrinsic behavior of CCTO because back-to-back barriers should give symmetrical I vs V curves, as observed in the Au/CCTO/LNO set-up. In addition, Ramirez *et al.* reported recently that CCTO thin films prepared on a Au/CCTO/Pt set-up at low temperatures (500-600 $^{\circ}\text{C}$) do not exhibit rectifying behavior in current-voltage measurements.³⁰ Moreover, our results show that the CCTO film prepared on a LNO buffer layer displays an ohmic contact with bottom (LNO) and top (Au) electrodes, and the sensor characterization reveals that CCTO film prepared by the PPM has n-type conductivity. Thus, our hypothesis is that the top (Au) electrode forms an ohmic contact, and the bottom (Pt) electrode and CCTO film form a MS rectifying interface influenced by the annealing temperature.

Keeping in mind the few studies about current charge transport in the CCTO/Pt interface and disregarding the resistive switching effect in the CCTO (discussed in Sec. III C), we resort to standard Schottky barrier theory in our discussion of the rectifying behavior limiting our assumptions to the current transport by the thermionic emission process and the

Schottky effect in a MS junction. The barrier potential height Φ_B formed between a metal and an n-type semiconductor can be given by:³⁵

$$\Phi_B = \Phi_M - \chi_s \quad (1)$$

where Φ_M is the work function of the metal and χ_s is the electron affinity of the semiconductor.

This relation is for the barrier height of an ideal Schottky barrier where surface states are neglected. If surface states are considered, the barrier height will depend upon both the metal work function and surface states on the semiconductor.³⁶ The Schottky-barrier height can be modified by image-force lowering (the Schottky effect), i.e., it is directly influenced by an external electric field which controls the charge carrier conduction across the junction. Furthermore, when subjected to an external electrical field, the Schottky barrier is modified and the effective height barrier is reduced or increased depending on the biasing conditions.³⁶ The determination of the Schottky barrier height can be obtained by energy-activation measurements which is an important approach in the investigation of novel or unusual MS interfaces. This method is based on the determination of the height barrier by the saturation current (I_0) instead of the current density because the electrode contact area is often unknown. Thus, the current density for a Schottky barrier has the following relationship with the electrical field:³⁶

$$J = A^* T^2 \exp \left[-\frac{(\phi_B - \beta \sqrt{E})}{kT} \right], \quad (2)$$

where A^* is Richardson constant for the material, k is Boltzmann constant, T is the absolute temperature, Φ_B is barrier height formed at the interface region, and $\beta \sqrt{E}$ is a term-related Schottky effect given by

$$\beta \sqrt{E} = \sqrt{\frac{E}{4\pi\epsilon_s}}, \quad (3)$$

where ϵ_s is the relative permittivity and E is the external electric field. The β term can be extracted from the slope of the I vs $E^{1/2}$ curve for a fixed temperature.³³ To obtain the barrier height of a CCTO/Pt junction, further analysis of the temperature dependence upon the saturation current is required using the relationship

$$\ln \left(\frac{I_0}{T^2} \right) = \ln(AA^*) - \frac{\phi_{B0}}{kT}, \quad (4)$$

where Φ_{B0} is the height barrier to $E=0$, and AA^* is the product of the electrically active area (A) and the effective Richardson constant (A^*).

Figure 5 shows the temperature dependence of the saturation current at the CCTO/Pt interface. The barrier height at this interface was calculated as 0.44 eV and the AA^* product is $8.90 \times 10^{-6} \text{ A.K}^{-2}$. This value is close to 0.46 eV as observed by Bodeux *et al.* for CCTO/Pt Schottky barriers using dc bias impedance measurements.³⁷ On the other hand, Deng *et al.*¹⁴ reported that CCTO thin films prepared by PLD have p-type conductivity and form a MS junction of

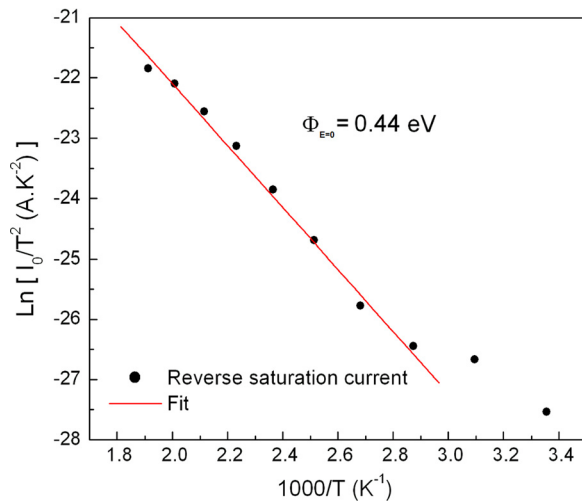


FIG. 5. Characteristic curve of $\text{Ln}(I_0/T^2)$ vs $1/T$ for a CCTO film deposited over Pt/Si substrate.

0.8 eV with the top (Pt) electrode prepared at room temperature. The difference between these CCTO/Pt interfaces can be related to two parameters:³⁶ (1) the conductivity type (n-type in our films); and (2) the formation temperature of the MS junction (775 °C in our films). In addition, in the case of an ideal Schottky barrier (Eq. (1)) and based on the work function values of platinum ($\Phi_{\text{Pt}} = 5.65$ eV) and the potential barrier height (0.44 eV), an electron affinity of up to 5.21 eV for CCTO thin films can be expected. Therefore, if the electron affinity of CCTO is close to the gold work function ($\Phi_{\text{Au}} = 5.10$ eV) and the conductivity of this sample is n-type, we can confirm that the formation of a MS junction occurs between the bottom (Pt) electrode and the CCTO film. This result confirms results reported by Bodeux *et al.* for CCTO thin films prepared by PLD with n-type conductivity using an Au/CCTO/Pt set-up which displays only one Schottky barrier at the CCTO/Pt interface due to the annealing process in the bottom Pt-electrode.³⁷

In addition (as discussed above), the effective barrier height of MS junctions depends on polarization; i.e., in a forward bias, there is an increase in the current across the interface due to a decrease in the barrier height while for the reverse bias, the barrier height increases and current across the interface decreases. I vs. V curves of the CCTO/Pt interface were simulated for forward and reverse bias at room temperature (Figure 6) based on constants determined experimentally ($\beta_r = 2.89 \times 10^{-4}$ eV $\text{cm}^{1/2} \text{V}^{-1/2}$ and $\beta_f = 4.47 \times 10^{-4}$ eV $\text{cm}^{1/2} \text{V}^{-1/2}$ for 25 °C and $AA^* = 8.90 \times 10^{-6}$ A.K^{-2}) and the Schottky thermionic emission equation (Eq. (2)). The simulations show that the best settings for effective barrier height values in the forward and reverse bias is 0.42 eV and 0.45 eV, respectively; i.e., lowering the forward bias height barrier by 0.02 eV and increasing the reverse bias height barrier by 0.01 eV. Best fitted curves (red line) and experimental data are illustrated in Figures 4 and 6. The fitted curves show good agreement between experimental and simulated data in reverse voltage and high forward voltage but not in low forward voltage. The charge transport in MS interfaces formed by high-mobility semiconductors can be better described by thermionic-emission theory, while the diffusion theory is bet-

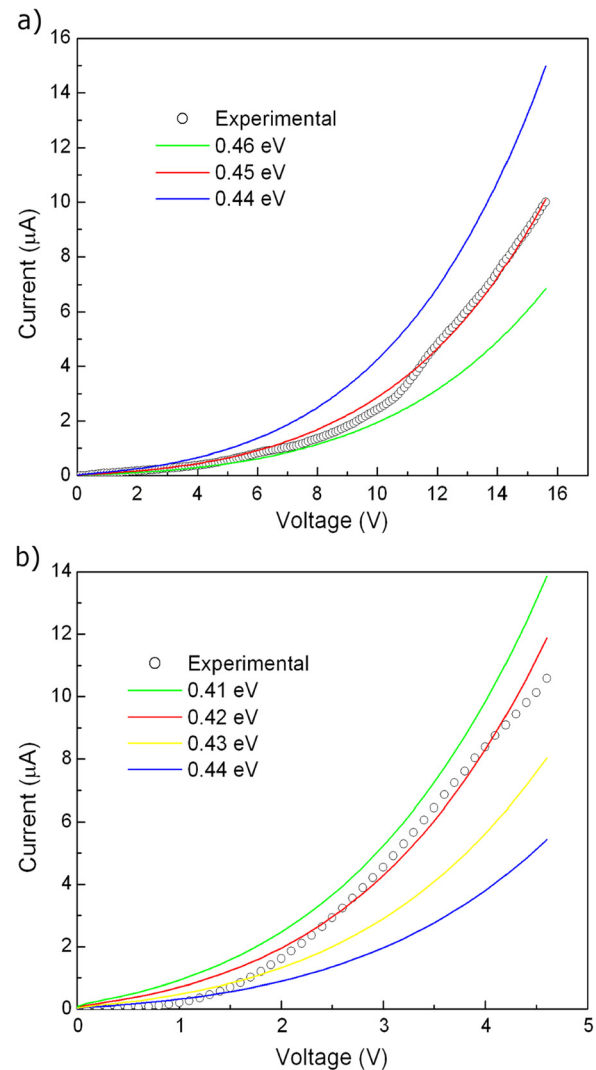


FIG. 6. Theoretical simulation of the Schottky diode behavior to (a) reverse and (b) forward current across of the CCTO/Pt interface.

ter applied to low-mobility semiconductors.³⁶ Furthermore, CCTO possesses both characteristics (low and high charge mobility) depending on the external applied field.^{30,34} Thus, these results indicate that the main transport mechanism in CCTO/Pt interfaces can be described by the thermionic-emission theory at high voltages due to the high charge mobility of CCTO. On the other hand, the diffusion theory could describe better the main transport mechanism due to the low charge mobility of CCTO at low voltages. Additional studies are necessary for the thermionic-emission-diffusion theory which we expect will produce a better fitting.³⁶

In summary, our results indicate that CCTO is a complex material, and its electrical properties are highly dependent on the synthesis route and electrode set-ups used in the device manufacturing. N-type CCTO thin films were obtained using the PPM which can have symmetrical or non-symmetrical non-ohmic behavior depending on the electrode set-up used. Using Au as a top electrode and LNO as a bottom electrode, ohmic contact is formed between the film and the electrodes, while using annealed Pt as a bottom electrode produces a rectifying MS junction. Current-voltage curves were fitted using a thermionic emission theory which

indicates that more than one mechanism can be involved in the current charge transport in CCTO/Pt interfaces.

C. Resistive switching effect

In the recent years, large efforts have been made to understand the resistive switching effects in metal-semiconductor materials, but the mechanisms responsible for these effects are not completely understood. In this context, aside from enrolling CCTO as a material candidate in this field, we would like to investigate the role of the electrode-CCTO interface and barrier contact on the resistive switching effects. Cyclic voltammetry measurements on Au/CCTO/LNO samples show two distinct resistance states for a voltage sweep range of -25V to 25V at a sweep rate of 500mV/s (see Figure 7). The measurement displays a hysteretic current-voltage profile with a $R_{\text{on}}/R_{\text{off}}$ ratio of 1.1. No change in the hysteretic behavior was observed relative to the voltage sweep or test electrodes. Current-voltage curves for CCTO prepared on a Pt bottom electrode at an equal sweep rate were performed; test electrodes and polarity configurations as well as voltage sweep (from -5V to $+5\text{V}$ and vice versa) are shown in Figure 8. The rectifying effect is independent of the current direction because the change of the electrode configuration (1 and 2) does not change the current direction; i.e., the direction of high current flow in the CCTO/Pt interface is dependent on polarity configurations due to the Schottky contact and is always higher from the Pt-electrode to the film than in the opposite direction. These results show an increased hysteretic current-voltage profile with a $R_{\text{on}}/R_{\text{off}}$ ratio of 3.2 and reveal a factor up to of three-fold increase in the $R_{\text{on}}/R_{\text{off}}$ ratio for the Au/CCTO/Pt set-up as compared to Au/CCTO/LNO set-up. Au is the top electrode in both samples forming ohmic contact. However, the bottom electrodes (LaNiO₃ and Pt) have different work functions, and contact barriers at bottom electrode/film interfaces are different, because LNO forms an ohmic contact and Pt forms a Schottky contact which could be causing different

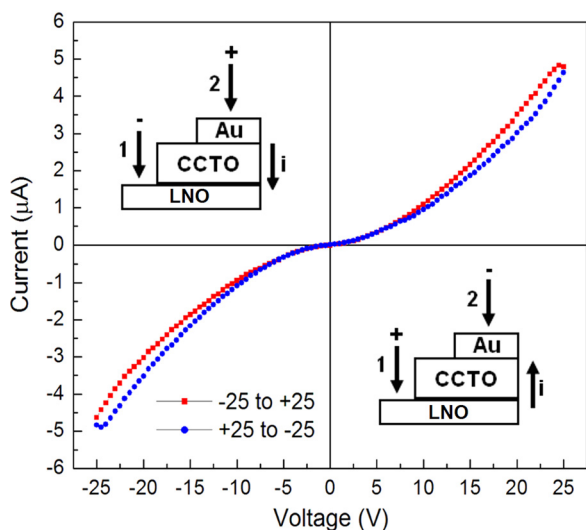


FIG. 7. Cyclic voltammetry curves of CCTO film deposited on LNO buffers. Measurements were performed by switching the test electrode (1 and 2) on the bottom and top electrodes; arrows in the Au/CCTO/LNO capacitor configuration indicate the current flow direction in both insets.

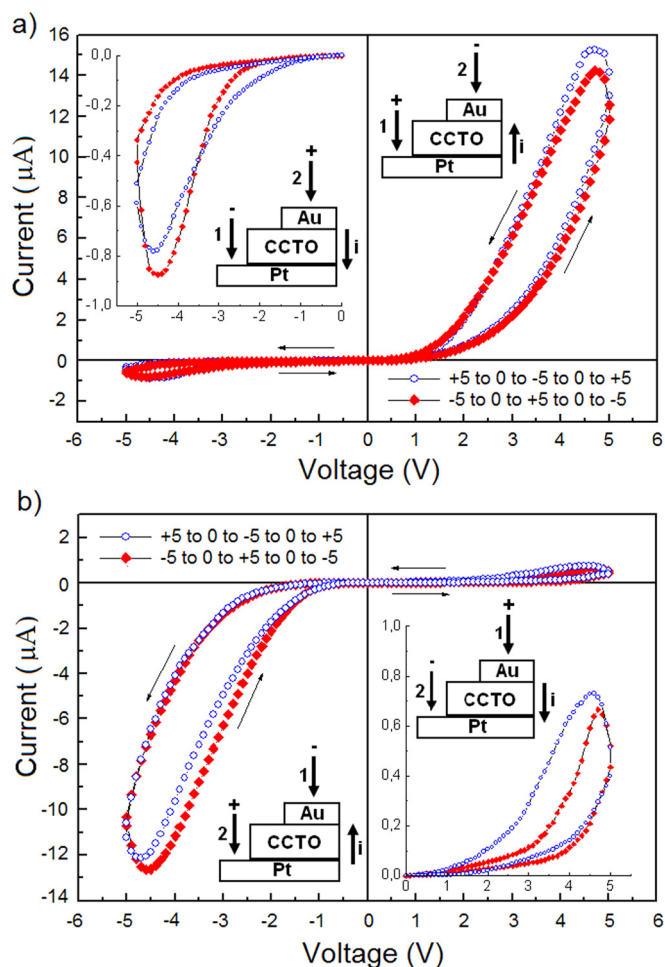


FIG. 8. Cyclic voltammetry curves of CCTO film deposited on Pt/Si substrate. Measurements were performed with switching the test electrode (1 and 2) on the bottom (a) and top (b) electrodes and the arrows in the Au/CCTO/Pt capacitor configuration indicate the current flow direction in all insets. The plot inset shows the zoom in the high resistance state.

screen electric fields at the bottom electrode/film interface. Thus, the formation of the Schottky contact increases the difference between the low and high resistance states as a consequence of an increase in the current flow in the forward voltage which results in a shift in the hysteresis loop and an enhanced resistive switching effect. Our results clearly indicate that the resistive switching effect in CCTO thin films is influenced by the barrier contact and the work function difference between CCTO and electrodes where metal electrodes with high work function values forming Schottky contacts can produce increased hysteresis and $R_{\text{on}}/R_{\text{off}}$ ratio.

In general, Schottky contacts in CCTO films may be beneficial for the electronic charge transport in resistance random access memory applications; and, on the other hand, the conductive oxides as electrical contact can result in an inferior resistive switching effect. However, additional studies are necessary to determine which mechanisms are responsible for the enhanced resistive switching behavior in CCTO/Pt interfaces.

IV. CONCLUSION

$\text{CaCu}_3\text{Ti}_4\text{O}_{12}$ (CCTO) thin films were prepared by PPM on different substrates, and electrical transport properties were characterized. Sensor response and thermopower

measurements reveal that CCTO films have n-type conductivity with high oxygen sensitivity. Films prepared on Pt/Si substrates show a rectifying behavior as a consequence of the formation of a MS junction between the bottom (Pt) electrode and the CCTO film. Films deposited on a LNO buffer or Pt/Si substrates indicate that the resistive switching effect in CCTO films depend upon the work function of the electrode and the type of contact formed. All experiments point to the strong influence of the oxide/electrode interface on the non-linear charge transport in CCTO thin films where the gas sensing, resistive switching, or rectifying characteristics may be enhanced depending upon the oxide/electrode set-up used.

ACKNOWLEDGMENTS

The authors gratefully acknowledge the financial support of the Brazilian foment agencies: FAPESP (Grant No. 2009-00367-6) and CNPq (Grant No. 200703/2011-0), and Swiss National Research Foundation for fellowship PP00P2-138914/1.

- ¹C. C. Homes, T. Vogt, S. M. Shapiro, S. Wakimoto, and A. P. Ramirez, *Science* **293**, 673 (2001).
- ²T. T. Fang, L. T. Mei, and H. F. Ho, *Acta Mater.* **54**, 2867 (2006).
- ³M. A. Subramanian, D. Li, N. Duan, B. A. Reisner, and A. W. Sleight, *J. Solid State Chem.* **151**, 323 (2000).
- ⁴A. P. Ramirez, M. A. Subramanian, M. Gardel, G. Blumberg, D. Li, T. Vogt, and S. M. Shapiro, *Solid State Commun.* **115**, 217 (2000).
- ⁵D. C. Sinclair, T. B. Adams, F. D. Morrison, and A. R. West, *Appl. Phys. Lett.* **80**, 2153 (2002).
- ⁶T. B. Adams, D. C. Sinclair, and A. R. West, *Adv. Mater.* **14**, 321 (2002).
- ⁷T. B. Adams, D. C. Sinclair, and A. R. West, *Phys. Rev. B* **73**, 094124 (2006).
- ⁸M. A. L. Cordeiro, F. L. Souza, E. R. Leite, and A. J. C. Lanfredi, *Appl. Phys. Lett.* **93**, 182912 (2008).
- ⁹X. J. Luo, C. P. Yang, S. S. Chen, X. P. Song, H. Wang, and K. Baerner, *J. Appl. Phys.* **108**, 014107 (2010).
- ¹⁰Y. S. Shen, B. S. Chiou, and C. C. Ho, *Thin Solid Films* **517**, 1209 (2008).
- ¹¹R. Tararam, E. Joanni, R. Savu, P. R. Bueno, E. Longo, and J. A. Varela, *ACS Appl. Mater. Interfaces* **3**, 500 (2011).
- ¹²Y. S. Shen, S. S. Ho, and B. S. Chiou, *J. Electrochem. Soc.* **156**, 466 (2009).
- ¹³G. Deng, Z. He, and P. Muralt, *J. Appl. Phys.* **105**, 084106 (2009).
- ¹⁴G. Deng, T. Yamada, and P. Muralt, *Appl. Phys. Lett.* **91**, 202903 (2007).
- ¹⁵E. Joanni, R. Savu, B. Jancar, P. R. Bueno, and J. A. Varela, *J. Am. Ceram. Soc.* **93**, 51 (2010).
- ¹⁶C. C. Lin, Y. P. Chang, C. C. Ho, Y. S. Shen, and B. S. Chiou, *IEEE Trans. Magn.* **47**, 633 (2011).
- ¹⁷I. D. Kim, A. Rothschild, T. Hyodo, and H. L. Tuller, *Nano Lett.* **6**, 193 (2006).
- ¹⁸R. Parra, R. Savu, L. A. Ramajo, M. A. Ponce, J. A. Varela, M. S. Castro, P. R. Bueno, and E. Joanni, *J. Solid State Chem.* **183**, 1209 (2010).
- ¹⁹E. Joanni, R. Savu, P. R. Bueno, E. Longo, and J. A. Varela, *Appl. Phys. Lett.* **92**, 132110 (2008).
- ²⁰S. M. Zanetti, E. B. Araujo, E. R. Leite, E. Longo, and J. A. Varela, *Mater. Lett.* **40**, 33 (1999).
- ²¹J. L. G. Fierro, *Metal Oxides: Chemistry and Applications* (Taylor & Francis, Boca Raton, 2006), Chap. 22.
- ²²S. R. Morrison, *The Chemical Physics of Surfaces* (Plenum, 1977).
- ²³D. E. Williams, *Sens. Actuators B* **57**, 1 (1999).
- ²⁴A. Gurlo, *ChemPhysChem* **7**, 2041 (2006).
- ²⁵W. Sun, H. Liu, W. Gong, L.-M. Peng, and S.-Y. Xu, *J. Appl. Phys.* **110**, 083709 (2011).
- ²⁶T. Suzuki, I. Kosacki, and H. U. Anderson, *Solid State Ionics* **151**, 111 (2002).
- ²⁷J. L. M. Rupp, B. Scherrer, and L. J. Gauckler, *Phys. Chem. Chem. Phys.* **12**, 11114 (2010).
- ²⁸F. D. Morrison, D. C. Sinclair, and A. R. West, *J. Am. Ceram. Soc.* **84**, 474 (2001).
- ²⁹S. Y. Chung, I. D. Kim, and S. J. L. Kang, *Nature Mater.* **3**, 774 (2004).
- ³⁰M. A. Ramirez, A. Z. Simões, A. A. Felix, R. Tararam, E. Longo, and J. A. Varela, *J. Alloys Compd.* **509**, 9930 (2011).
- ³¹H. Han, J. Zhong, S. Kotru, P. Padmini, X. Y. Song, and R. K. Pandey, *Appl. Phys. Lett.* **88**, 092902 (2006).
- ³²M. S. Hegde, K. M. Satyalakshmi, R. M. Mallya, M. Rajeswari, and H. Zhang, *J. Mater. Res.* **9**, 898, 1994.
- ³³A. A. Felix, M. O. Orlandi, and J. A. Varela, *Solid State Commun.* **151**, 1377 (2011).
- ³⁴G. Zang, J. Zhang, P. Zheng, J. Wang, and C. Wang, *J. Phys. D.: Appl. Phys.* **38**, 1824 (2005).
- ³⁵E. H. Rhoderick and R. H. Williams, *Metal-Semiconductor Contacts* (Clarendon, Oxford, 1988).
- ³⁶S. M. Sze, *Physics of Semiconductor Devices* (Wiley, New York, 1981).
- ³⁷R. Bodeux, M. Gervais, J. Wolfman, C. A. Lambert, G. Liu, and F. Gervais, *Thin Solid Films* **520**, 2632 (2012).